Spectral Decomposition of a T-7A Red Hawk Installed GE F404 Engine

Cooper Merrill

A capstone report submitted to the faculty of
Brigham Young University
in partial fulfillment of the requirements for the degree of

Bachelor of Science

Kent Gee, Advisor

Department of Physics and Astronomy

Brigham Young University

ABSTRACT

Spectral Decomposition of a T-7A Red Hawk Installed GE F404 Engine

Cooper Merrill
Department of Physics and Astronomy, BYU
Bachelor of Science

Better phenomenological noise source models for full scale military aircraft can enhance current noise mitigation efforts for military aircraft. Similarity spectra analysis is a common method for identifying both the fine-scale and large-scale spatial components of jet noise. For an imperfectly expanded supersonic jet, the addition of a broadband shock-associated noise model helps to better fit the spectral shape of measured full scale jet noise. A similarity spectra analysis of T-7A-installed GE-F404 engine noise has been performed at intermediate to full afterburner conditions. The broadband shock-associated noise contributions are significant for military and afterburner conditions. The combined model captures the noise reasonably well with some caveats. First, spatiospectral lobes present in the measured noise are not well represented. Second, the measured low-frequency spectral slope is steeper at higher engine conditions in the region of maximum radiation. Third, the measured high-frequency slope is shallower across most of the radiation angles. Fourth, the noise at large inlet angles, beyond the peak radiation lobe, is not well represented by the combined model. The successes and failures of this model for different spatial regions and frequencies will aid in developing improved models for noise radiation.

ACKNOWLEDGMENTS

I would like to thank the Brigham Young University Department of Physics and Astronomy for the quality instruction I have received in my core classes as an undergraduate student. My professors have all helped me to learn challenging concepts. I have been inspired during my time as a physics student at BYU to go forth to serve after graduation.

I would like to thank Dr. Kent Gee for mentoring me and investing time in me in his research group. I feel that my experience studying jet noise has prepared my more than any other singular activity at BYU for my future career. Participating in the research process has been the most difficult and most rewarding part of my undergraduate experience.

I would like to thank my parents for supporting me during my studies at BYU. I would especially like to thank my father who inspired me to study physics and to conquer my hardest challenges through endurance and tenacity. Finally I would like to thank my wife for her incredible support and patience through the long days and late nights of my studies.

Contents

List of Figures

Chapter 1

Introduction

1.1 Motivation

Noise reduction efforts for full-scale military aircraft are of increasing importance for military and civilian communities. Aircrew working in the run-up area are subject to high amplitude noise which can cause damage to hearing and complicate aircraft run-up, taxi, and takeoff procedures. Communities surrounding military air bases experience significant noise pollution from aircraft. A better understanding of different noise components and the development of phenomenological noise models relevant for full-scale military aircraft will benefit the development of noise mitigation technologies [1].

1.2 Similarity Spectra Analysis

Similarity spectra analysis is a popular method of analyzing noise source components in jet noise research. The goal of similarity spectra analysis is to decompose a noise source into its dominant frequencies. If the dominant frequencies of a noise source are known, we can sum sine waves with these frequencies together to approximate the original signal to a great degree of accuracy. At the

core of similarity spectra analysis is the Fourier Transformation. This is a process which takes a signal in the time domain and converts it to the same signal in the frequency domain; instead of having a plot of a signal as a function of time F(t), we have a plot of our signal as a function of frequency F(w). The frequencies with the highest amplitudes are the dominant frequencies in the signal being studied. This process is known generally as Fourier analysis or spectral analysis. This is helpful because different noise sources may be associated with different frequency bands. Knowing the dominant frequencies gives us insight into the main physical sources of the signal.

In jet noise, rather than seeing a few distinct dominant frequencies in the Fourier transform of the time domain signal, we see a distribution of a large range of frequencies. Similarity spectra are functions which approximate the frequency domain signal F(w) of a known noise source. These similarity spectra can be fit to the frequency domain signal F(w) of a measured noise source. Fitting these similarity spectra for across a spatial microphone array gives insights into the the locations of noise sources and the directions of radiation for these sources. This process also gives insight into the relative levels of these noise sources. Understanding how a signal is generated enables the noise source to be modeled and predicted. These models and predictions are crucial in designing active and passive mitigation measures for a given signal. The process of fitting similarity spectra to measured noise spectra is called similarity spectra analysis.

1.3 Three Source Model

Large-scale mixing noise (LSN), fine-scale mixing noise (FSN) and broadband shock-associated Noise (BSN) account for a majority of the noise generated from military aircraft [2]. Large-scale turbulent structures on the outside of the jet plume interact with ambient air to produce LSN which radiates downstream [3]. Fine-scale structures also interact with ambient air producing low-level noise which radiates in all directions [3]. Shock-associated noise is comprised of BSN and screech

tones. Screech is a component of supersonic jet noise related to the presence of shock cells in a jet. In turbulent jets, the shear layers interact with the shock cells resulting in screech, a tonal noise significant in lab scale jets. Screech, while important in underexpanded lab-scale jets, does not contribute significantly to full-scale jet noise [3]. Because military aircraft are overexpanded at field elevations, BSN is significant at high engine powers. BSN is caused by interactions between large-scale turbulent structures and shock cells [4] and radiates to the sideline and upstream of the jet [3].

Similarity spectra developed from lab-scale jets can be used to model large-scale and fine-scale mixing noise, and broadband shock-associated noise. Although these spectra were developed for lab-scale jets they have been successfully applied to measurements of full-scale military aircraft [2, 5]. LSN and FSN require two parameters to fit measured spectra, peak frequency and peak level. BSN requires a third parameter relating to the width of the spectra to be fit to measured spectra. Tam *et al.*'s large-scale Spectra $L_L(F)$ and fine-scale Spectra $L_F(F)$ [6] together with Kuo *et al.*'s BSN model $L_B(F)$ [4], can be added together to create a combined model $L_T(F)$ which captures measured noise from a full-scale jet remarkably well. However previous studies have consistently found a few discrepancies between the modeled and measured spectra including multiple spectral peaks at intermediate to afterburner engine conditions, low frequency errors in the region of maximum radiation at high engine conditions, and high frequency slope disagreement at most inlet angles [2, 5, 7].

This thesis uses Tam *et al.*'s mixing noise model [6], and Kuo *et al.*'s BSN model [4] to perform a near-field three-way spectral decomposition on a GE-F404 jet engine installed on a T-7A Redhawk. A description of the measurement is followed by an analysis of the efficacy of the three-source model to describe the noise generated by the T-7A trainer aircraft. Results are shown for 75% thrust, and afterburner engine conditions. The successes of this model for different spatial regions and frequencies demonstrate the ability of the three-source model to capture the general spectral shape

of full-scale jet noise. The failures of this model to capture the details of the spectral shape of full-scale jet noise indicate a need for further study of noise source mechanisms in order to fully model noise from full-scale military aircraft.

Chapter 2

Methods

2.1 Overview

The T-7A Red Hawk has been selected as the replacement of the T-38 Talon as the United States Air Force's new trainer for fighter and bomber pilots. Its single GE F404-103 engine produces approximately 11,000 lbf of thrust without afterburner and 17,000 lbf at afterburner. Variants and derivatives of this engine have been used in other full scale military aircraft. The three main purposes of the measurement were to characterize the noise for environmental and community impact, understand noise levels experienced by maintainers close to the aircraft, and increase the understanding of the noise generated by full-scale military aircraft. A full description of the measurement is given in [8] but relevant details for this paper are included here.

2.2 Measurement Environment

The measurement was taken under the leadership of the Air Force Research Laboratory (AFRL) in the early morning at Holloman Air Force Base on August 18th, 2019 from 0500 to 0700 local time to avoid high wind speeds. The temperature was between 19.9° and 25.8° C, the humidity was

5

between 21.9 and 31.9% and the average wind speed during the measurement was 1.9 kts. The aircraft was tied to a concrete pad extending 40 feet from both sides of the aircraft. The concrete pad extended far downstream. The aircraft nose was pointed towards the jet blast deflector as can be seen in Fig. 2.1 to decrease noise reflections and provide a further area downstream where measurements could be taken.

This paper focuses on data taken from 120 microphones in a near-field array. This array was placed along the left side of the aircraft, but the Fig. 2.2 mirrors the array on the right side for plotting convenience. Microphone locations are given in distance from the nozzle in the aft and sideline directions and angle relative to the microphone array reference position (MARP). The MARP is in the jet center line 13 feet downstream from the nozzle. The near field array utilized both GRAS 1/4" 46 BG and 46 BD pressure and 46 BE free-field microphones. The 46 BE microphones were pointed toward the MARP, while the 46 BG and BD microphones were perpendicular to the MARP. Microphones were taped to the ground to reduce ground reflection interference. Spacing between microphones was based on predicted peak frequencies. The microphones were placed closer together where higher frequencies were expected to dominate, and further apart where low frequencies were expected to dominate. The average microphone spacing was closer than previous measurements of military aircraft to allow finer spatial resolution and frequency bandwidth analysis.

2.3   Measurement Procedure

Military aircraft are operated at idle all the way up to afterburner on the ground during the engine start, runup, and takeoff sequences, so it is important to understand the noise generated at low and high engine power conditions. The aircraft was cycled through several engine conditions six times resulting in six separate runs at each engine condition. Data was recorded for at least 30 seconds during each run. The engine was set to idle for a few minutes after afterburner before

Figure 2.1 T-7A tied to concrete pad with nose facing jet blast deflector at Holloman AFB.
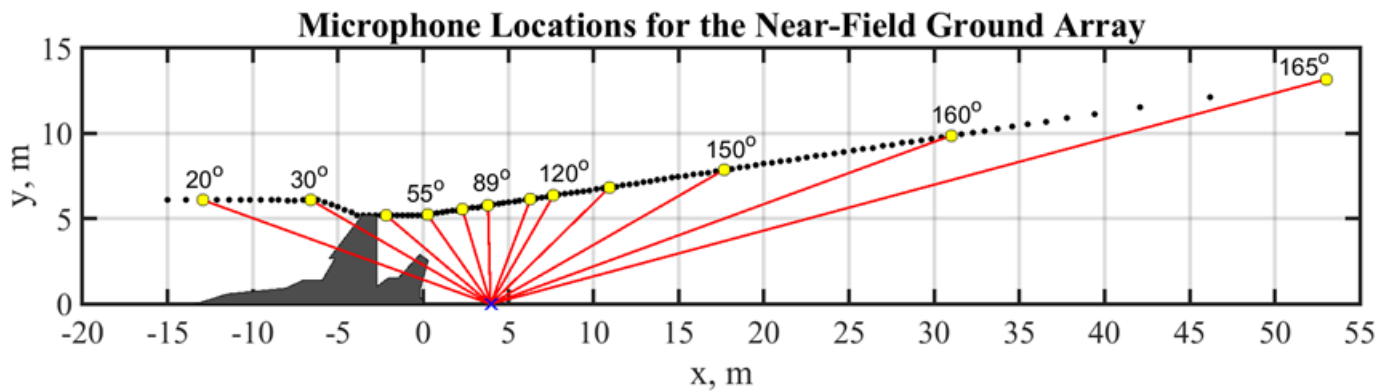

Figure 2.2 Top view looking down on the near Field Microphone Array with distance in meters and angles shown from the MARP. Black dots represent microphones with red lines to yellow dots showing specific angles for reference. Microphone Array Reference Point (MARP) is represented by a blue cross.

cycling through the engine conditions again. This letter will focus on 75% thrust and full afterburner conditions. These engine conditions capture the major trends in full-scale military aircraft important to evaluating the efficacy of the three-source model. The 24 bit National Instruments PXIe system was used for all 120 microphones with a sampling rate of 204.8 kHz and a +/- 10 Volt range. IRIG-B GPS time clocks allowed for the recordings to be synchronized in post-processing.

2.4   Data Processing

To analyze the contributions of various noise sources, the similarity spectra developed for mixing noise and broadband shock-associated noise developed from lab-scale jet databases [4, 6] were manually fit by committee to the measured spectra. Before fitting the measured spectra for each microphone, the average of the six runs was taken at 50% thrust, 75% thrust, military power, and afterburner for each microphone. Modeled spectra were then fit to the average sound level curves for the average of the six runs at each microphone. These fits were scrutinized and improved several times over. In cases where more than one similarity spectrum was needed to fit the measured noise, the sum of the similarity spectra used was computed to model the noise. Fitting decisions were made to best capture the overall sound pressure levels, to fit the peak of the measured spectra, and to smoothly vary the parameters of the modeled spectra. This method was previously used successfully in Neilsen *et al.* [2]. Fitting modeled spectra to measured data is the foundation of the analysis to follow.

Chapter 3

Results

3.1 Overview

The three-source model captures the sound levels produced by an installed GE F404 engine reasonably well. The model accounts for the measured noise within a few dB across a wide range of angles and frequencies. However, there are some limitations. The model does not capture the multiple spectral peaks seen at some angles in the measured spectra. There are also significant low frequency errors at afterburner in the region of maximum radiation, and high frequency errors across most of the radiation angles at all engine conditions. In addition, the noise far downstream at large inlet angles is not well represented.

3.2 Individual Spectra

Individual spectral fits are the core of the analysis to follow. As the following spectral decompositions show, the majority of the spectral shape across the microphone array can be represented with a combination of Kuo *et al.*'s BSN model, and Tam *et al.*'s mixing noise model. Examples of similarity spectra fits for 75% thrust and Afterburner are shown in Fig. 3.1.
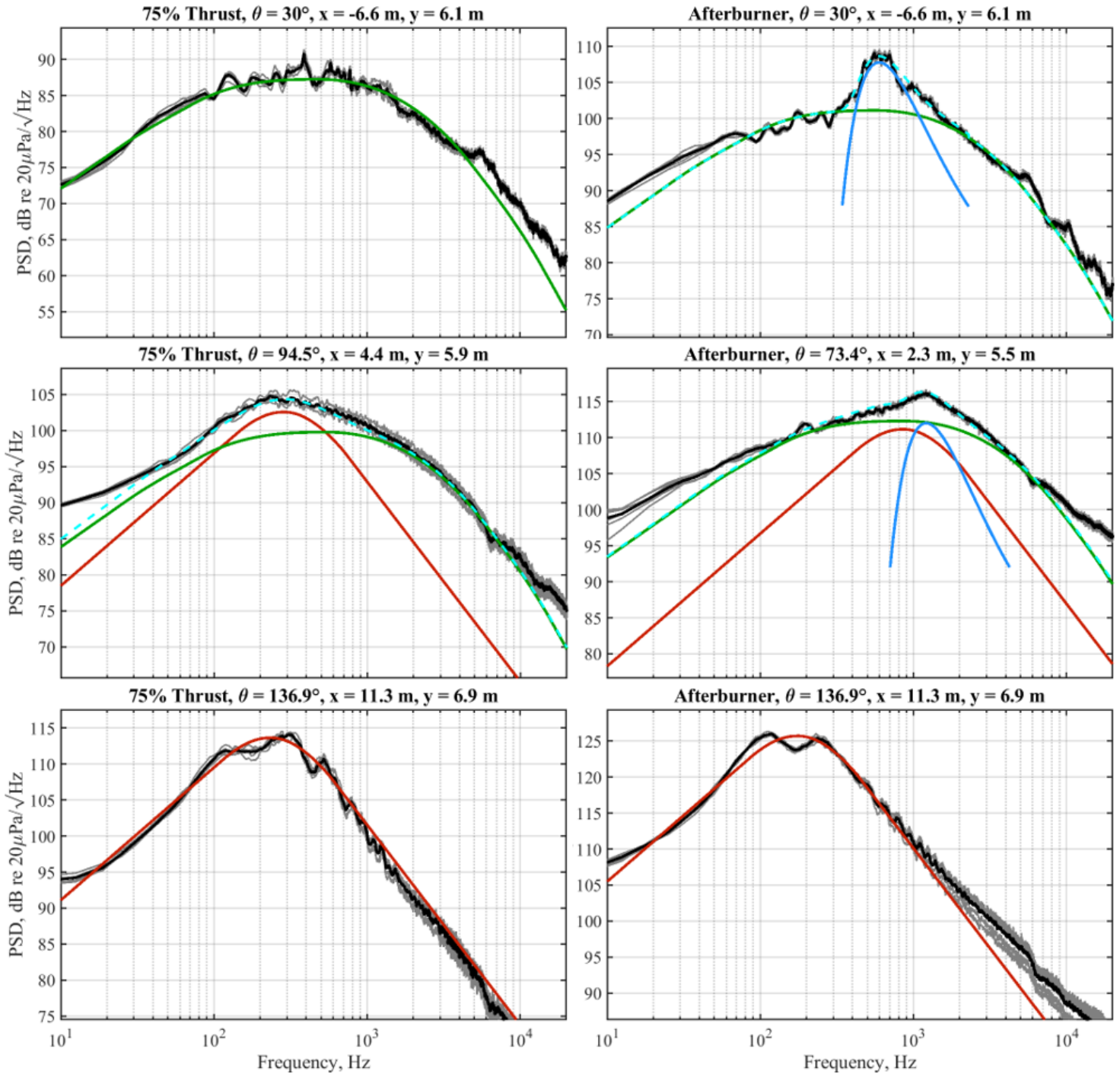
Figure 3.1 Selected Spectral fits at 75% thrust (left) and afterburner (right) engine conditions. Average sound level is plotted as a function of frequency and modeled spectral fits are shown. Green shows fine-scale spectra, red shows large-scale spectra, blue shows BSN, and dashed cyan shows the sum of the modeled spectra.
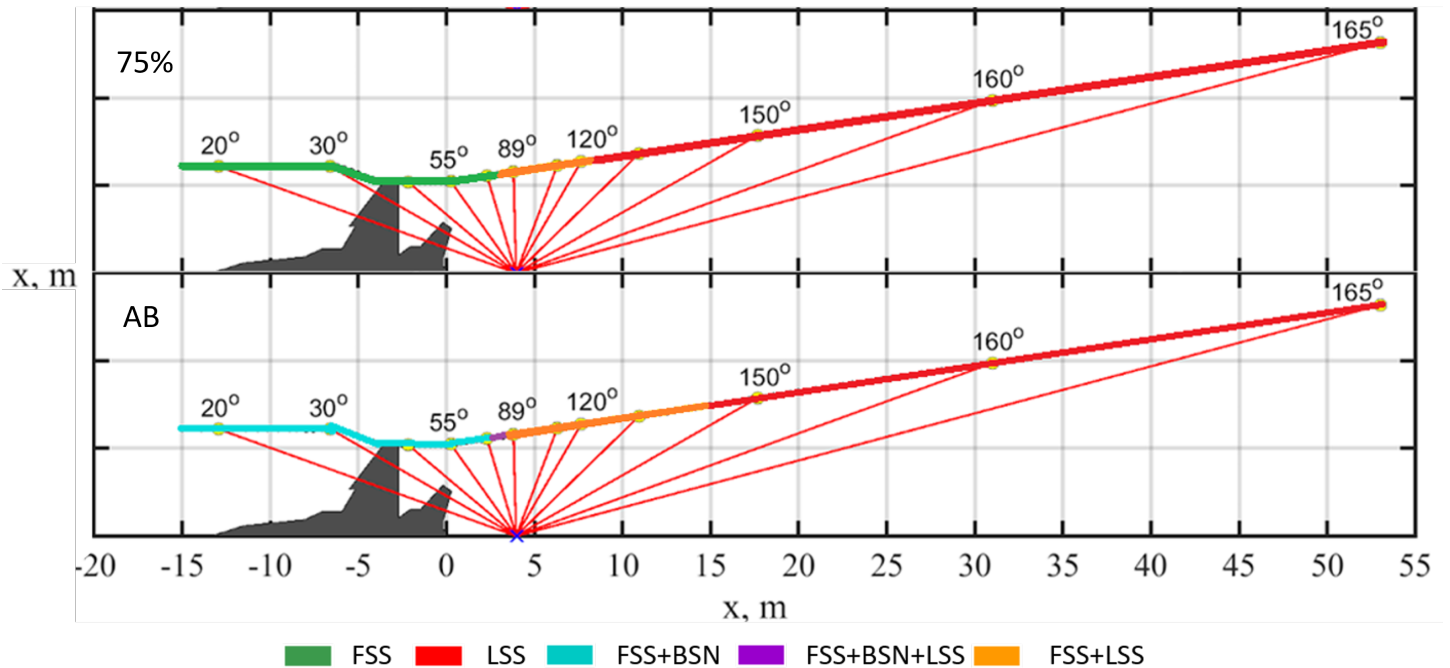
Figure 3.2 Spectra location indicated by color on the Microphone Array for 75% thrust (top) and afterburner (bottom).

Fig. 3.1 shows that the three-source model captures the spectral shape of the measured noise at 75% thrust and afterburner over a wide range of angles, but with the caveats mentioned previously. At 136.9° multiple spectral peaks which cannot be captured by the model are seen at both engine conditions. Additionally, at afterburner at 136.9°, the measured low-frequency slope is steeper than the model predicts. At both engine conditions, the high-frequency slope is shallower than the model predicts at most radiation angles.

Fine scale mixing noise, large scale mixing noise, and broadband shock associated noise similarity spectra curves were used to fit the measured noise at different ranges of angles from the MARP. Fig. 3.2 shows where each similarity spectra were used to fit the data.

Fig. 3.2 and Fig. 3.3 show that FSN is dominant upstream of the jet to just before the sideline of the MARP. BSN is present for afterburner everywhere FSN is present. There is not evidence in the data of BSN where FSN does not contribute significantly to the OASPL. LSN becomes significant

around 88° for 75% thrust and around 74° for afterburner. At afterburner, there is a small region where FSN, LSN, and BSN all contribute significantly to the OASPL. Both engine conditions transition from a region where FSN dominates to a region dominated by LSN. For afterburner this happens further upstream, at around 85°. This also occurs around 105° for 75% thrust. These trends are consistent with the findings of Vaughn *et al.* [3].

There are several trends for BSN seen in Fig. 3.4 and Fig. 3.3. First, the peak frequency of the $L_B(F)$ increases as inlet angle increases. This is consistent with the lab-scale jets and with the large eddy simulations by Liu *et al.* [9] where increasing BSN peak frequency in the near-field corresponded to a decrease in shock cell size. The peak level of $L_B(F)$ also increases with inlet angle until 62° after which the peak level begins to decrease slightly. In addition the width of the $L_B(F)$ spectra is constant from the beginning of the array to approximately 40°. Between 40 and 62° the width of $L_B(F)$ decreases. After 62° it increases until there is no longer significant evidence of BSN around 85°. These trends are consistent with those observed by Neilsen *et al.* [2]. Tam *et al.* [5] also found that peak frequency increases with inlet angle. However the peak level was not observed to decrease with increasing inlet angle at any point, and the width of the $L_B(F)$ spectra was only seen to decrease with increasing inlet angle. Significantly, the trends for the peak level and spectral width in lab-scale jets are opposite to those seen in Tam *et al.* [5], Neilsen *et al.* [2], and in the T-7A analysis.

3.3   Overall Sound Pressure Level

Fig. 3.3 shows the general success of the three-source model. Mixing noise and BSN together account for the measured sound levels of the jet remarkably well, within a few dB. Additionally the shape of the OASPL curve for afterburner and 75% thrust are very similar to each other. The OASPL curves for both engine conditions follow roughly the same trends with the afterburning

engine condition producing significantly more noise. The sound pressure levels for afterburner are as much as 20 dB higher at afterburner than 75% thrust. The sound pressure levels are also disproportionately elevated for afterburner between 15° and 85° due the the presence of BSN wich is absent for 75% thrust. Errors are most significant at small angles relative to the MARP, and far downstream at large angles from the MARP. While Fig. 3.3 shows that the model captures the OASPL of the measured noise well, it is not particularly helpful for understanding how well the model produces the correct spectral shape of the noise across the microphone array. To successfully model the noise we need to mimic both OASPL and the spectral shape. Spatiospectral difference maps of the measured noise minus the calculated noise can help us see trends in how the $L_T(F)$ fits across the microphone array.

3.4   Spatiospectral Maps

The spatiospectral maps show good agreement between the modeled noise and the measured noise over a wide range of angles and frequencies. As seen in Fig. 3.3 the difference between the measured and modeled noise is within +/- two dB over a large range of frequencies and inlet angles. However these maps show trends in the ability of the model to match the spectral shape and show the caveats seen in the individual spectra in Fig. 3.1. In these areas the errors are significantly larger than +/- two dB.

Spatiospectral lobes are present in both engine conditions. These lobes show up in the difference maps as a pattern of positive and negative errors at larger inlet angles between 100 and 1,000 Hz. These lobes are due to a pattern of over and underestimation by the three-source model caused by multiple spectral peaks in measured noise. These lobes were also prominent in Nielsen *et al.* [2] and were found at both 75% thrust and afterburner. At afterburner, there is some significant error in the low frequencies in the region of maximum radiation due to the low-frequency spectral slope
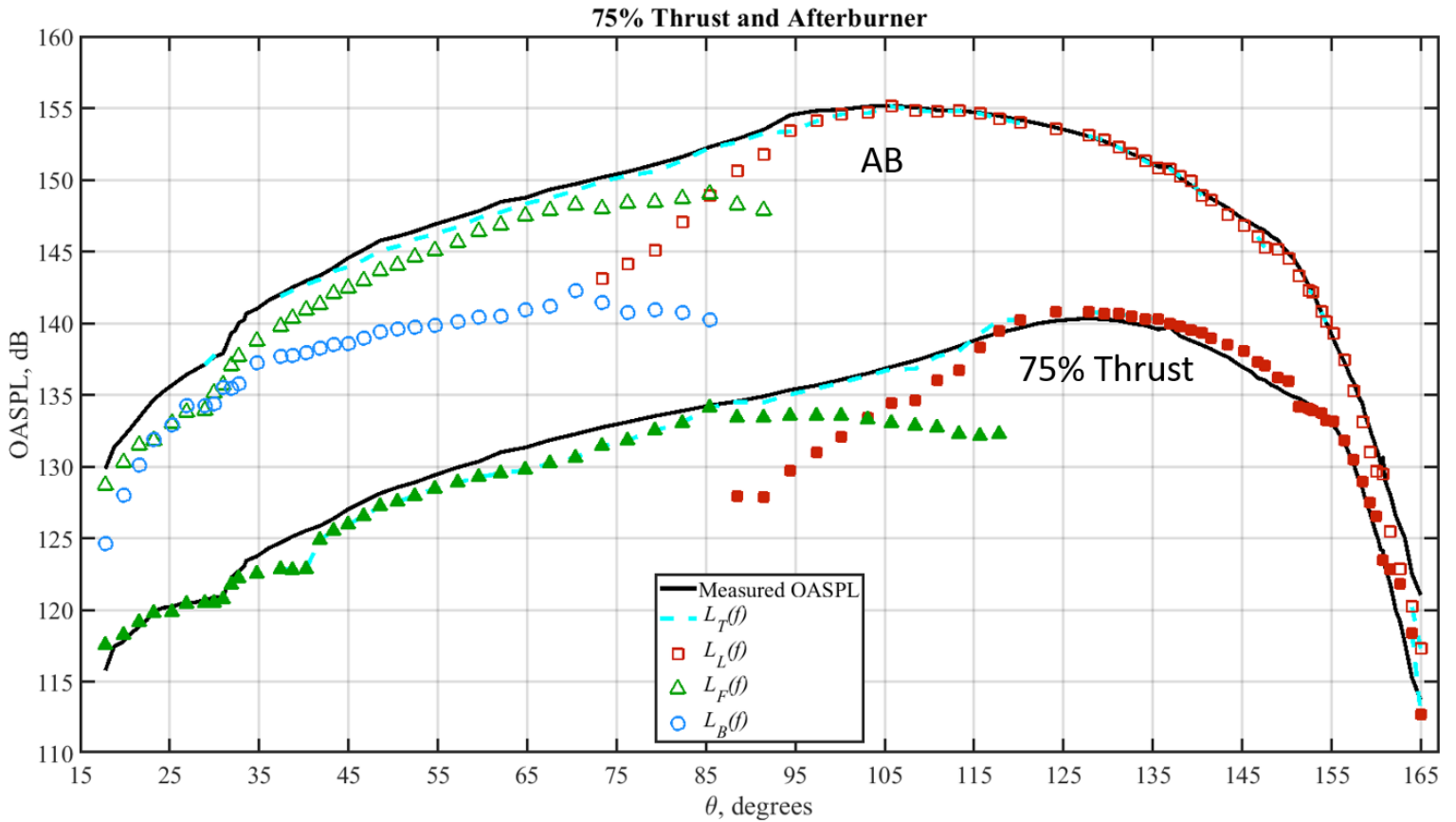
Figure 3.3 Overall sound pressure level (OASPL) as a function of angle from the MARP For afterburner and 75% thrust engine conditions. Green triangles represent the Fine Scale Spectra contributions, red squares represent Large Scale Spectra contributions, blue circles represent Broadband Shock Associated Noise contributions, and the dashed blue represents the sum of all the contributions and the modeled overall sound pressure level.
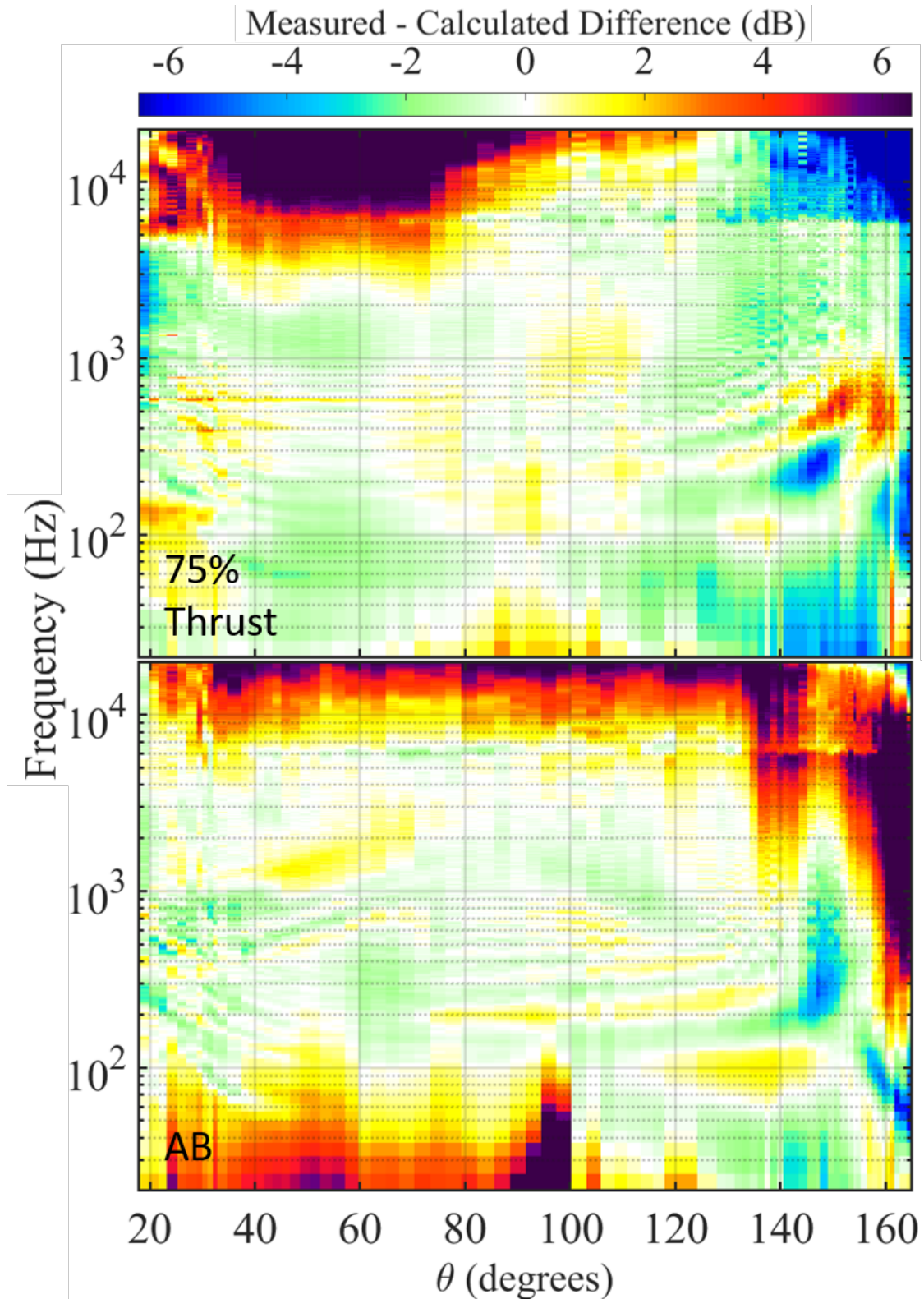
Figure 3.4 Difference maps between measured and modeled sound levels as a function of frequency in Hz and angle from the MARP in degrees for both 75% thrust (top) and Afterburner (bottom).

being steeper than the model predicts in this region. The very high errors between 90° and 100° are in part caused by microphone saturation effects in the low frequencies below 100 Hz, but are also due to the low-frequency spectral slope being steeper at higher engine conditions in the region of maximum radiation. BSN is modeled effectively for the afterburning engine condition and there are no significant errors due to BSN. Additionally, there are significant high-frequency errors in both engine conditions. This is because the measured high-frequency slope is shallower than the modeled slope across most of the radiation angles. $L_F(F)$ was not used to help fit this shallower slope at higher inlet angles because the shallower spectral slope is approximately 20 dB/decade which is indicative of by nonlinear propagation effects, [10] and there is not significant evidence for the presence of FSN this far downstream of the aircraft nozzle. Finally, individual spectra towards the end of the microphone array show significant errors at large inlet angles beyond the peak radiation lobe because the measured noise is not represented well by the combined model in this region. This was not found in previous studies in the near-field ground array; however the near-field ground microphone array in this study extended further downstream than previous studies. The large variability between runs for these large inlet angles indicates that hydrodynamic effects are likely responsible for the failure of the $L_L(F)$ to fit the measured noise well. The general shape of the spectra at these large angles still resembles the shape of LSN. These errors, while small are important because they demonstrate that we cannot fully capture the spectra of full-scale jet noise from similarity spectra developed for lab-scale jets. These caveats have been consistently observed in previous studies of full-scale military aircraft [2, 5, 7].

3.5   Conclusion

Similarity spectra analysis is an important tool in breaking down full-scale military aircraft noise. This decomposition of a T-7A installed GE-F404 demonstrates the ability of the three-source model

to capture the overall sound pressure level of full-scale jet noise, and to capture the general spectral shape of full-scale jet noise across a wide range of inlet angles and frequencies; however there are some small but consistent errors across several studies of full scale military aircraft that are physically significant. Data from the T-7A experiment displays multiple spectral peaks in addition to high and low frequency errors. Due to these discrepancies $L_T(F)$ does not fully capture the spectral shape of full-scale jet noise. This is consistent with previous studies of military aircraft [2, 5, 7]. Similarity spectra analysis using similarity spectra developed from lab-scale jets [4, 6] for mixing noise and BSN has not fully captured the details of the spectral shape of full-scale military aircraft noise in several studies [2, 5, 7]. This suggests that there are noise source mechanisms in full-scale military aircraft that are not present or not significant in lab-scale jets. Moreover, the trends for peak level and the spectral width of $L_B(F)$ for the T-7A and other full-scale military aircraft are opposite those for lab-scale jets [2]. This is additional evidence that there there are important physical differences between lab-scale and full-scale jets. Similarity spectra developed from lab-scale jets can capture the overall sound pressure level and the general spectral shape of full-scale military jets, however, these spectra cannot fully model the noise generated by full-scale military aircraft. Understanding these mechanisms is necessary to create a model that can fully capture the spectral shape of military aircraft noise. Such a model will enhance the efficacy of jet noise mitigation efforts. Mitigation of full-scale tactical aircraft noise is important for the health of maintainers working around the aircraft during the run-up sequence, and for the communities around the operational area of these aircraft. Further study and analysis are needed to identify these mechanisms and provide a more complete model for full-scale jet noise.

Bibliography

[1] D. Casalino, F. Diozzi, R. Sannino, and A. Paonessa, "Aircraft noise reduction technologies: A bibliographic review," Aerospace Science and Technology **12,** 1–17 (2008).

[2] T. B. Neilsen, A. B. Vaughn, K. L. Gee, S. H. Swift, A. T. Wall, J. M. Downing, and M. M. James, "Three-Way Spectral Decompositions of High-Performance Military Aircraft Noise," AIAA Journal **57,** 3467–3479 (2019).

[3] A. B. Vaughn, T. B. Neilsen, K. L. Gee, A. T. Wall, J. Micah Downing, and M. M. James, "Broadband shock-associated noise from a high-performance military aircraft," The Journal of the Acoustical Society of America **144,** EL242–EL247 (2018).

[4] C.-W. Kuo, D. K. McLaughlin, P. J. Morris, and K. Viswanathan, "Effects of Jet Temperature on Broadband Shock-Associated Noise," AIAA Journal **53,** 1515–1530 (2015).

[5] C. K. Tam, A. C. Aubert, J. T. Spyropoulos, and R. W. Powers, "On the Dominant Noise Components of Tactical Aircraft: Laboratory to Full Scale," In *23rd AIAA/CEAS Aeroacoustics Conference*, (American Institute of Aeronautics and Astronautics, Denver, Colorado, 2017).

[6] C. Tam, M. Golebiowski, and J. Seiner, "On the two components of turbulent mixing noise from supersonic jets," In *Aeroacoustics Conference*, (American Institute of Aeronautics and Astronautics, State College,PA,U.S.A., 1996).

[7] T. B. Neilsen, K. L. Gee, A. T. Wall, and M. M. James, "Similarity spectra analysis of high-performance jet aircraft noise," The Journal of the Acoustical Society of America **133,** 2116–2125 (2013).

[8] K. M. Leete, A. B. Vaughn, M. S. Bassett, R. D. Rasband, D. J. Novakovich, K. L. Gee, S. C. Campbell, F. S. Mobley, and A. T. Wall, "Jet Noise Measurements of an Installed GE F404 Engine," In *AIAA Scitech 2021 Forum*, (American Institute of Aeronautics and Astronautics, VIRTUAL EVENT, 2021).

[9] J. Liu, A. T. Corrigan, K. Kailasanath, N. S. Heeb, and E. J. Gutmark, "Numerical Study of Noise Sources Characteristics in An Underexpanded Jet Flow," In *20th AIAA/CEAS Aeroacoustics Conference*, (American Institute of Aeronautics and Astronautics, 2014).

[10] T. B. Neilsen, K. L. Gee, A. T. Wall, M. M. James, and A. A. Atchley, "Comparison of supersonic full-scale and laboratory-scale jet data and the similarity spectra for turbulent mixing noise," In , pp. 040071–040071 (Montreal, Canada, 2013).

Index